J Mater Sci: Mater Electron (2015) 26:9200–9204
DOI 10.1007/s10854-015-3612-0

Phase transition and energy storage performance in Ba-doped PLZST antiferroelectric ceramics

Xiucai Wang[1,2] · Jie Shen[1] · Tongqing Yang[1,2] · Zhao Xiao[1] · Ying Dong[1]

Received: 4 April 2015 / Accepted: 8 August 2015 / Published online: 18 August 2015

Abstract $(Pb_{0.97-x}Ba_xLa_{0.02})(Zr_{0.7}Sn_{0.27}Ti_{0.03})$ $(0 < x < 0.08)$ antiferroelectric (AFE) ceramics were successfully fabricated by a solid state reaction, and the effect of barium (Ba) additions and temperature on the dielectric properties and energy storage performance were investigated. The ceramics with lower Ba content undergo two phase transitions during heating from room temperature to 300 °C: orthorhombic (O)-rhombohedral (R)-cubic (C). With the increase of Ba content, dielectric constants increased and transition temperature decreased obviously. The ferroelectric phase was induced as the composition x increased from 0 to 0.08, however, which was not stable and transformed into AFE state upon heating, and then paraelectric phase, which was confirmed by DC field dependence of dielectric constant. The polarization sharply increased from 9.7 μC/cm^2 at 20 °C to 24. 6μC/cm^2 at 100 °C in $(Pb_{0.89}Ba_{0.08}La_{0.02})(Zr_{0.7}Sn_{0.27}Ti_{0.03})$ ceramic. As a result, the maximum recovered energy density of 2.1 J/cm^3 was obtained at 80 °C, and the corresponding energy-storage efficiency was 76.5 %, which made this material a promising potential application in capacitors for pulsed power systems.

✉ Tongqing Yang
yangtongqing@tongji.edu.cn

[1] Key Laboratory of Advanced Civil Engineering Materials (Ministry of Education), Functional Materials Research Laboratory, College of Materials Science and Engineering, Tongji University, 4800 Cao'an Road, Shanghai 201804, China

[2] Functional Materials Research Laboratory, College of Materials Science and Engineering, Tongji University, Shanghai, China

1 Introduction

Lead zirconate titanate (PZT) and its related materials are widely used in high-power energy storage, cooling device and pulsed power systems due to their excellent field induced phase transitions and composition-tunable dielectric properties [1–4]. The dipoles in AFEs are alternatively aligned in the opposite directions, and no macroscopic spontaneous polarization exists [5]. The AFE phase can be transformed to the FE phase when the applied electric field is above the threshold electric field (E_{AF}); the FE state can return to the AFE state when the field decreases to the threshold electric field (E_{FA}), and this process is often accompanied by larger strains and polarization changes [6, 7]. Moreover, AFEs also possess faster charge–discharge speed and excellent fatigue endurance owing to their unique field-induced AFE–FE phase switching [8]. Chen [9] showed the discharge property of slanted ceramics with energy storage density 0.31 J/cm^3, and pulse current peak could reach 1.8 kA at 40 kV/cm.

It was very difficult for AFE ceramic to withstand a large external field. In order to tailor the dielectric properties, A- and B-site compositional modifications in PLZST system with a ABO_3 perovskite-structure were usually employed [10, 11]. Recoverable energy density (W_{re}) of 61 J/cm^3 with an efficiency of 33 % had been demonstrated in AFE PLZT thin films under an applied field of ≈4.3 MV/cm [12]. However, the energy density of AFE ceramics were usually <2 J/cm^3 in previous studies due to lower dielectric polarization and lower break-down strength [13, 14]. Zhang [15] studied the effect of barium content on energy storage properties of $(Pb,La,Ba)(Zr,Sn,Ti)O_3$ ceramics in tetragonal phase and the maximum energy storage density of 0.7 J/cm^3 was obtained.

In this study, Ba-doped PLZST ceramics in orthorhombic region were fabricated by the conventional solid state reaction route, and the temperature dependence of phase transition, electrical properties and energy storage performance were investigated. The polarization and energy storage exhibited great sensitivity to temperature, the maximum recovered energy density was up to 2.1 J/cm^3 with an efficiency of 76.5 %. In addition, DC field dependence of dielectric constant at different temperature were also studied.

2 Experimental procedure and methods of data analysis

$(Pb_{0.97-x}Ba_xLa_{0.02})(Zr_{0.7}Sn_{0.27}Ti_{0.03})$ (x = 0, 0.04, 0.08) (abbreviated as B0, B4, B8, respectively) ceramics were prepared via methods of the solid state reaction with raw materials PbO_2(99.0 %), $BaCO_3$(99.0 %), TiO_2(99.0 %), ZrO_2(99.0 %), SnO_2(99.5 %) and La_2O_3(99.99 %). The mixed powders were calcined at 900 °C for 2 h. The calcined powders were mixed with addition of alcohol again, dried and pressed into 10 mm diameter pellets and sintered at 1230 °C for 3 h. Silver electrodes were fired on both surfaces of the specimens for electric measurement.

The sample crystallization behavior was examined by X-ray diffraction meter (XRD, D8 Advance; Bruker AXS GmbH, Karlsruhe, Germany); Dielectric properties were characterized with precise LCR meters from 1 to 1000 kHz in the temperature range 20–300 °C at a rate of 2 °C/min (HP 4284A and HP 4294A; Hewlett Packard Co, Beijing, China); Polarization–electric field (P–E) loops were characterized with a precision ferroelectric analyzer (Premier II, Radiant Technologies Inc.) combined with a high voltage power supply (TReK Model 663A) for pellets placed in a silicone oil bath setup at different temperature. A lab-established computer controlled ε–E analyzer system which includes an LCR meter (TH2816; Tonghui Electronic Instrument Corp., Changzhou, China), a high-voltage generator (YJ93A; Shanghai Scientific Instrument Research Institute, Shanghai, China), and a sample chamber.

3 Results and discussion

X-ray diffraction patterns of virgin samples (B0, B4, B8) at room temperature are shown in Fig. 1, and the index has been marked, and impurity peak is not detected with the increase of Ba content, indicating that all the ceramics have crystallized into a single perovskite phase after final annealing at 1230 °C for 3 h.

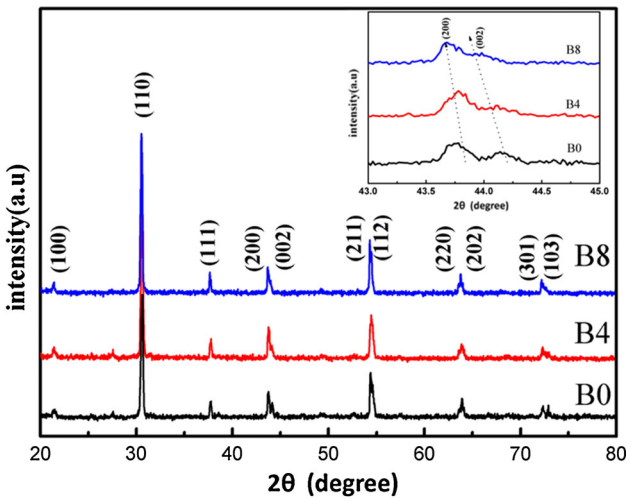

Fig. 1 XRD patterns of B0, B4 and B8 ceramics

Figure 2 shows dielectric constant (ε) of Ba-doped PLZST ceramics as a function of temperature and frequency, respectively. As shown in Fig. 2a, dielectric constant of all samples shows tremendous stability within frequency varies between 1 and 10 MHz, and share very small loss tangent of below 0.017, which is attributed to their uniform microstructure. As Ba content increases to 0.08, the dielectric constant increases from 390 to 720 at room temperature. Generally, the dielectric constant of AFE materials has a close relationship with the stability of AFE phase, and higher stability of the AFE phase usually leads to lower dielectric constant. From Fig. 2b, there are two anomalies (T_{m1} and T_{m2}) with lower Ba additions, indicating two phase transition on heating. T_{m1} occurs at 125 °C for B0, and it is confirmed that the ceramics undergo a first-order phase transition that orthogonal phase (O) to rhombohedral (R) phase when the amount of Ba is less in previous results [16]. It is interesting to note that the T_{m1} and T_{m2} decreases with Ba additions increasing, as Ba content increases to 0.08, the T_{m1} disappears within temperature range. The maximum dielectric constant for B0, B4, and B8 is 1150, 1216, and 1653, respectively.

The P–E of all samples at room temperature are presented in Fig. 3, and the scanning time in all P–E experiments is 10 ms. Because of different Ba content, there are significant differences in P–E loops. As shown, a classic double-hysteresis of AFE phase is observed without Ba additions, and AFE phase becomes less stable as Ba additions increases and prone to induce to FE phase. As x = 0.08, the sample becomes a FE phase and possesses a slim P–E loops with a small remnant polarization. Ba as a FE phase stabilizer should be responsible for the transformation.

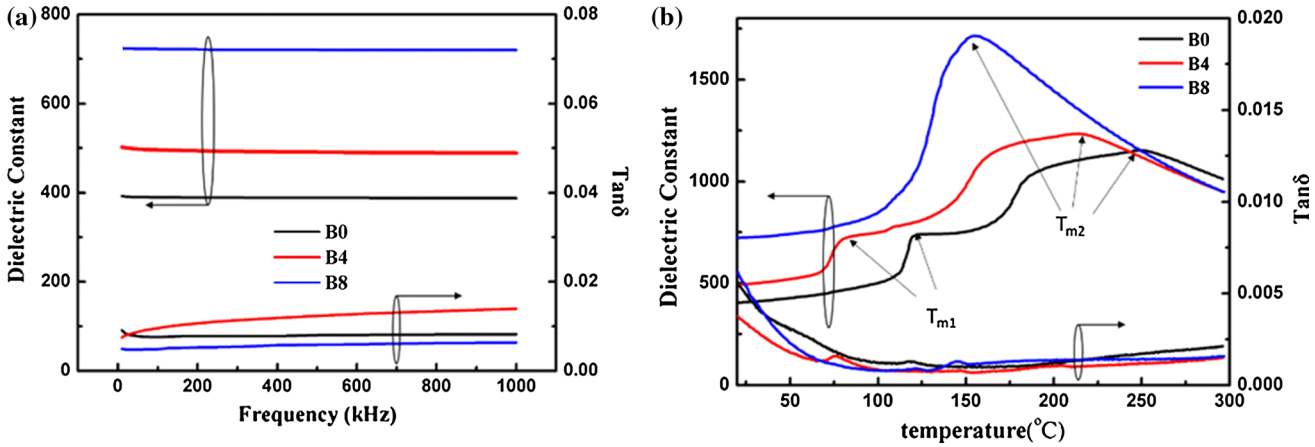

Fig. 2 Dielectric constant (ε) and tanδ of Ba-doped PLZST ceramics as a function of temperature and frequency

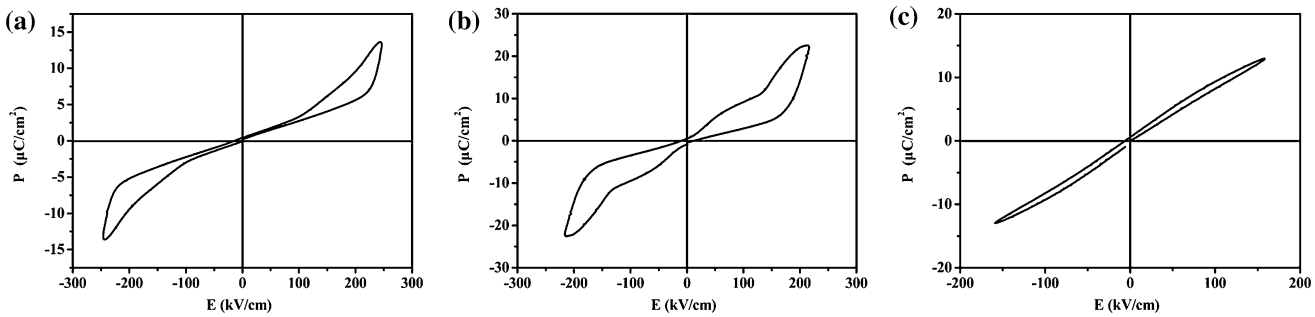

Fig. 3 Polarization hysteresis (P–E) loops of Ba-doped PLZST ceramics at room temperature. **a** B0, **b** B4, **c** B8

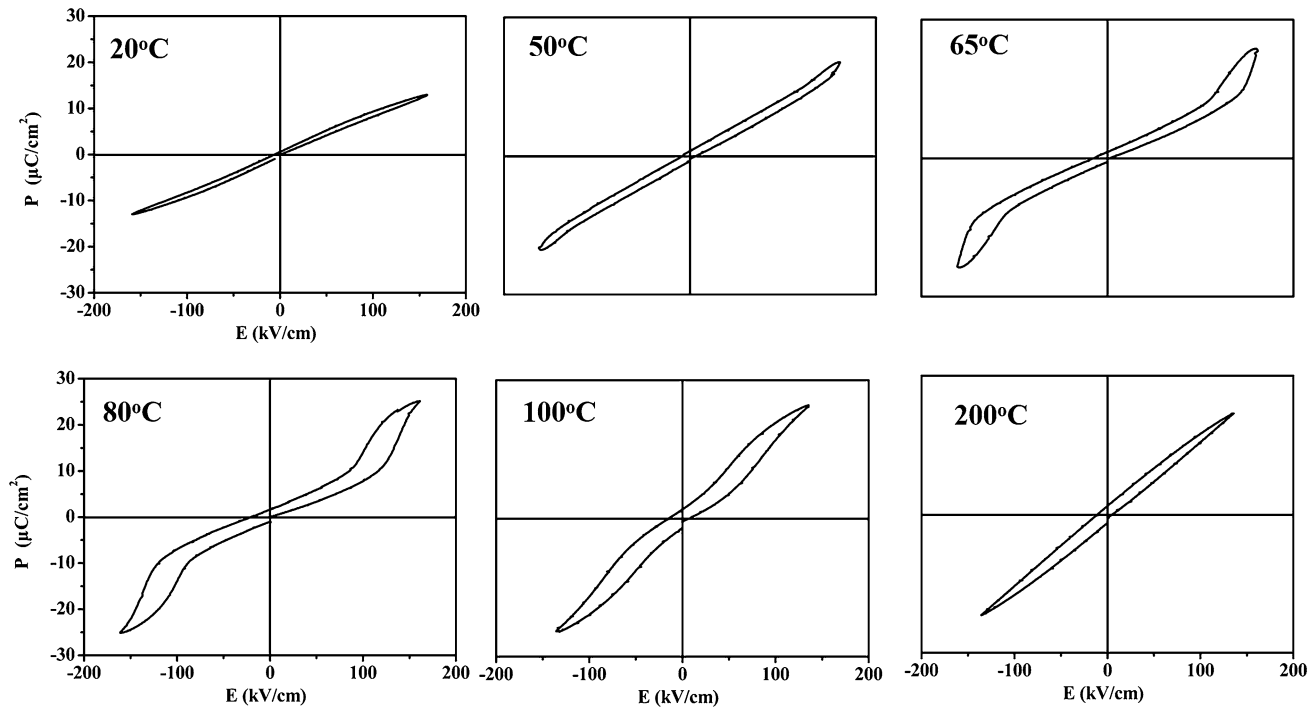

Fig. 4 The P–E behaviors of sample B8 under various temperatures

To evaluate the effect of temperature on B8, the P–E behaviors under various temperatures are plotted in Fig. 4. As we can see, the FE phase can exist when the temperature is below 20 °C, but then becomes a little AFE-like at 50 °C and transforms into a typical AFE phase with the temperature further increase, indicating that a FE–AFE phase transition. It is believed that the ground state of PLZST, and induced to AFE phase during particular temperature range. Chan [17] demonstrated the recovery to the AFE state was fast at high temperatures, which led to the typical AFE double P–E behavior. Furthermore, AFE domains disappear and linear P–E behavior becomes evident on further heating to or above T_C, indicating an AFE–PE transformation. As a consequence, B8 ceramic changes from FE to AFE and then PE phase as the temperature increases. The polarization initially slightly increases, and then undergoes a drastic fluctuation with the heating process (dramatically rise from 9.7 μC/cm^2 at 20 °C to 24.6 μC/cm^2 at 100 °C under 135 kV/cm), and quickly reduces to 10.9 μC/cm^2 at 200 °C, as shown in Fig. 6a. The polarization of Ba-droped PLZST becomes relatively sensitive to temperature, this may be caused material structure distortion by doping Ba, and thermal motion increases between A-site and B-site, resulting in a FE–AFE phase transition and a dramatic increase of polarization. The mechanism and more details still need further research in the future.

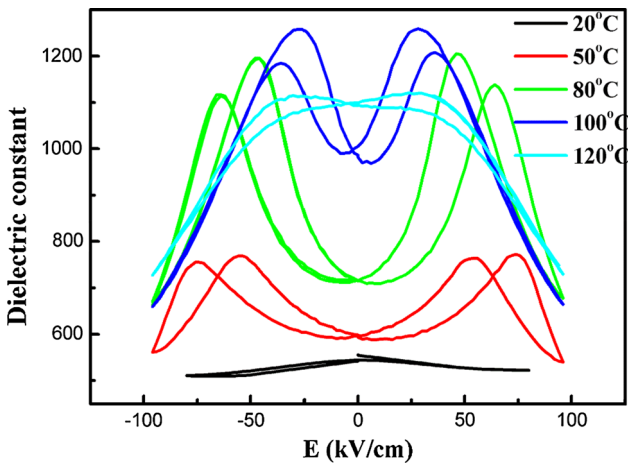

Fig. 5 DC field dependence of ε for B8 ceramics at different temperature

DC field dependence of ε for B8 ceramics at different temperature are shown in Fig. 5, electric constant decreases with increasing electric field at 20 °C, indicating that the B8 cerimics is a FE phase. At 50 °C, The dielectric constant is about 580 with E = 0 V/cm, and increases sharply with increasing electric-field, which demonstrates that the sample has changed from FE phase to AFE phase. Dielectric constant and the tunability gradually increases with the increase of temperature, proving that the AFE phase becomes more stable. DC field dependence of ε at different temperature is in conformity with the P–E loops of B8 ceramics, confirming that the temperature induced FE–AFE phase transition.

Figure 6b depicts temperature-dependent recovered energy density (W_{re}) and the efficiency (η) of B8 ceramics. The stored energy is only partially released, we calculate the stored energy density (W) and W_{re} from the P–E hysteresis loops measured under an electric field of 135 kV/cm at different temperatures. The W_{re} is obtained by numerical [18] integration of the area between the polarization axis and the back switching curve of the P–E loops. Because of the increasing polarization values, it can be found that the B8 ceramics possess higher W_{re} values with increasing temperature, and the maximum value is up to 2.1 J/cm^3 at 80 °C. Because of fluctuation of polarization, the W_{re}

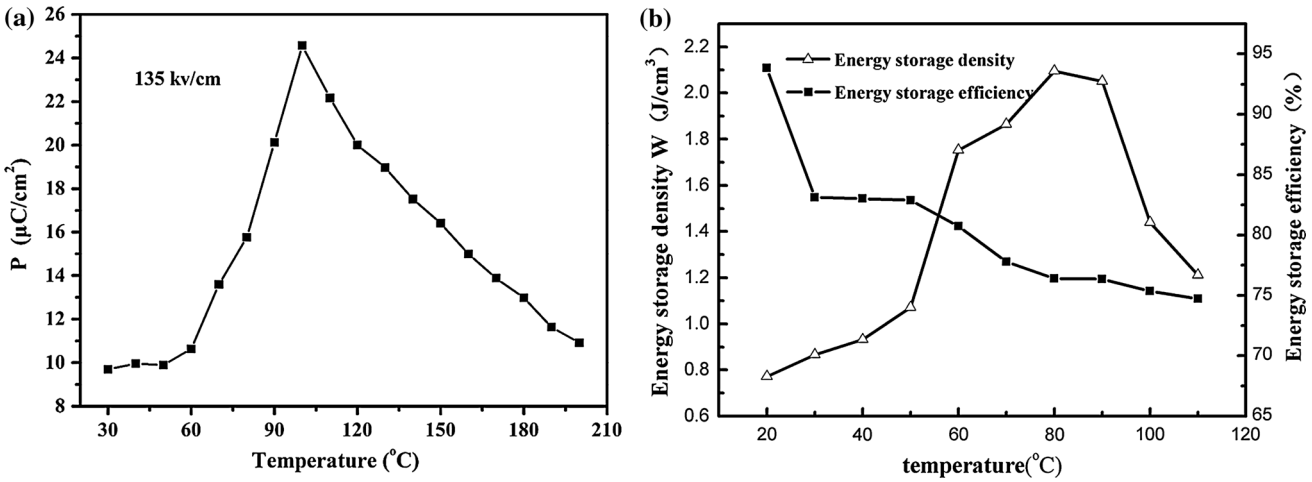

Fig. 6 Temperature-dependent **a** polarization and **b** recovered energy density and the efficiency of B8 ceramics

declines with the heating process. In the practical application, a higher η (or lower energy loss) is also desired, and the η could be calculated according to the formula: $\eta = W_{re}/W_{re} + W_{loss}$. The energy-loss density (W_{loss}) is calculated by numerical integration of closed area of the hysteresis loops. It can be seen that the η of B8 is also strongly influenced by temperature, sharply increases first, and then slightly decreases with increasing temperature. Clearly, the η_{max} of 93.82 % is obtained at 20 °C, indicating that the slim hysteresis loop is beneficial to increase the energy-storage efficiency. The polarization and energy storage performance are so sensitive to temperature, making it has a good application prospect in high-power energy storage and uncooled heat sensing applications.

4 Conclusions

Ba-modified PLZST ceramics were examined by the X-ray, dielectric constant, and P–E loops. The ceramics with lower Ba content undergone two transitions during heating from room temperature to 300 °C: orthorhombic (O)-rhombohedral (R) phase -cubic (C). The dielectric constant increased and the transition temperature decreased as the Ba additions increased. The nature state of $(Pb_{0.89}Ba_{0.08}La_{0.02})(Zr_{0.7}Sn_{0.27}Ti_{0.03})$ was a FE phase with a slim P–E loops, and changed to AFE above 50 °C, and finally PE phase with the temperature raised. This phase transition was confirmed by DC field dependence of dielectric constant. The polarization, W_{re} and η were strongly influenced by temperature. The polarization undergone a drastic fluctuation, and led to the W_{re} dramatically increased almost three times from 0.77 J/cm^3 at 20 °C to 2.1 J/cm^3 at 80 °C, and the corresponding efficiency was 76.5 %. This phenomenon were rarely involved in the previous report. Thus, it could be concluded that Ba-doped PLZST ceramics were suitable for uncooled heat sensing applications and high-power energy-storage.

Acknowledgments This work was supported by the National Natural Science Foundation of China (No. 51272178) and the Innovation Program of Shanghai Municipal Education Commission (No. 14ZZ041).

References

1. R. Lu, J. Yuan, Q.L. Zhao, B. Li, Y. Li, M.S. Cao, J. Mater. Sci. Mater. Electron. **24**, 2521 (2013)
2. K. Ramam, A.J. Bell, C.R. Bowen, K. Chandramouli, J. Alloys Compd. **473**, 330 (2009)
3. K. Markowski, S.E. Park, S. Yoshikawa, L.E. Cross, J. Am. Ceram. Soc. **79**, 3297 (1996)
4. R. Rai, S. Mishra, N.K. Singh, J. Alloys Compd. **487**, 494 (2009)
5. S.E. Park, K. Markowski, S. Yoshikawa, L.E. Cross, J. Am. Ceram. Soc. **80**, 407 (1997)
6. H. He, X.L. Tan, Phys. Rev. B **72**, 024102 (2005)
7. F. Xue, L.Y. Liang, Y.J. Gu, I. Takeuchi, S.V. Kalinin, L.Q. Chen, Appl. Phys. Lett. **106**, 012903 (2015)
8. X.F. Chen, H.L. Zhang, F. Cao, G.S. Wang, X.L. Dong, Y. Gu, H.L. He, Y.S. Liu, J. Appl. Phys. **106**, 034105 (2009)
9. X.F. Chen, F. Cao, H.L. Zhang, G. Yu, G.S. Wang, X.L. Dong, Y. Gu, H.L. He, Y.S. Liu, J. Am. Ceram. Soc. **95**, 1163 (2012)
10. A. Mesquita, A. Michalowicz, P.S. Pizani, K. Provost, V.R. Mastelaro, J. Alloys Compd. **582**, 680 (2014)
11. N. Zhang, Y.J. Feng, Z. Xu, Mater. Res. Innov. **15**, 240 (2011)
12. Z. Hu, B. Ma, R.E. Koritala, U. Balachandran, Appl. Phys. Lett. **104**, 263902 (2014)
13. Q.F. Zhang, M.W. Fan, S. Jiang, T.Q. Yang, J.F. Wang, X. Yao, J. Alloys Compd. **551**, 279 (2013)
14. J.F. Wang, T.Q. Yang, S.C. Chen, G. Li, Mater. Res. Bull. **48**, 3847 (2013)
15. Q. Zhang, X.L. Liu, Y. Zhang, X.Z. Song, J. Zhu, I. Baturin, J.F. Chen, Ceram. Int. **41**, 3030 (2015)
16. Y.Y. Li, Q. Li, Q.F. Yan, Y.L. Zhang, X.Q. Xi, X.C. Chu, W.W. Cao, Appl. Phys. Lett. **101**, 132904 (2012)
17. W. Chan, Z. Xu, J.W. Zhai, E. Colla, H. Chen, J. Electron. Ceram. **21**, 145 (2008)
18. C. Cho, D.A. Payne, S. Cho, Appl. Phys. Lett. **71**, 3013 (1997)